Journal of Magnetic Resonance **145,** 307–314 (2000)
doi:10.1006/jmre.2000.2087, available online at http://www.idealibrary.com on IDEAL®

^{15}N Chemical Shift Tensor Magnitude and Orientation in the Molecular Frame of Uracil Determined via MAS NMR

Jörg Leppert, Bert Heise, and Ramadurai Ramachandran

Abteilung Molekulare Biophysik/NMR Spektroskopie, Institut für Molekulare Biotechnologie, D-07745 Jena, Germany

Received December 17, 1999; revised February 22, 2000

The potential of heteronuclear MAS NMR spectroscopy for the characterization of ^{15}N chemical shift (CS) tensors in multiply labeled systems has been illustrated, in one of the first studies of this type, by a measurement of the chemical shift tensor magnitude and orientation in the molecular frame for the two ^{15}N sites of uracil. Employing polycrystalline samples of $^{15}N_2$ and 2-^{13}C,$^{15}N_2$-labeled uracil, we have measured, via ^{15}N–^{13}C REDOR and ^{15}N–^{1}H dipolar-shift experiments, the polar and azimuthal angles (θ, ψ) of orientation of the ^{15}N–^{13}C and ^{15}N–^{1}H dipolar vectors in the ^{15}N CS tensor frame. The (θ_{NC}, ψ_{NC}) angles are determined to be (92 ± 10°, 100 ± 5°) and (132 ± 3°, 88 ± 10°) for the N1 and N3 sites, respectively. Similarly, (θ_{NH}, ψ_{NH}) are found to be (15 ± 5°, −80 ± 10°) and (15 ± 5°, 90 ± 10°) for the N1 and N3 sites, respectively. These results obtained based only on MAS NMR measurements have been compared with the data reported in the literature. © 2000 Academic Press

Key Words: **chemical shift tensors; dipolar couplings; MAS; solid-state NMR; REDOR.**

INTRODUCTION

An accurate knowledge of the magnitude and orientation of CS tensors has been found to be invaluable in the characterization of biomolecular structure and dynamics via NMR spectroscopy (*1–9*). Motivated by this, there have been extensive experimental investigations dealing with the study of, e.g., ^{15}N CS tensors of the amide fragment of peptides (*10*). Quantum chemical calculations are also being increasingly used to rationalize the relationship between chemical shift tensors and polypeptide structure (*11*). The importance of the knowledge of ^{15}N chemical shift tensors has also been pointed out recently in the context of the study of nucleic acids (*12–14*). From the studies reported in the literature it is seen that the ^{15}N CS tensor magnitude and orientation in the molecular frame may vary from site to site as well as for the same site within a class of similar compounds (*10, 15*). Hence, for reliable structural and dynamical investigations that require an accurate knowledge of the chemical shift tensors it may be necessary to determine these for each site of interest. In the characterization of chemical shift tensors, solid-state NMR has emerged as a powerful tool (*16*).

NMR measurements on single crystals allow the complete characterization of chemical shift tensors. However, due to the difficulties in growing large single crystals needed in these studies, techniques based on powder specimens are being increasingly used. In static solid-state NMR experiments the principal values of the ^{15}N CS tensor are obtained directly from ^{1}H decoupled static powder spectra and the orientational information is traditionally obtained from a study of the mutual orientation of the chemical shift and dipolar tensors (*17*). Due to severe spectral overlaps that one encounters in static solid-state NMR studies, such methods have limited utility in the study of multiply labeled systems. Several MAS NMR studies have been reported recently (*18–21*) for the characterization of chemical shift tensors in systems containing dipolar coupled homonuclear spin-1/2 pairs. In this work, we deal with systems containing three heteronuclear spin-1/2 nuclei (^{13}C, ^{15}N, ^{1}H). It is shown below that in multiply ^{15}N-labeled systems with resolved isotropic ^{15}N shifts, thanks to the improved spectral resolution and sensitivity obtainable, heteronuclear magic angle spinning solid-state NMR spectroscopy can be conveniently employed to fully characterize the chemical shift tensors. As part of our ongoing efforts on the characterization of CS tensor magnitude and orientations in nucleic acids, we have employed REDOR (*22–24*) and dipolar-shift (*25–27*) experiments in a study of [1,3–$^{15}N_2$ and 1,3-$^{15}N_2$,2-^{13}C]uracil, which is one of the four bases in RNA. The magnitudes of the chemical shift tensor principal values have been obtained via an analysis of the spectral sideband amplitudes of conventional ^{1}H decoupled CPMAS spectra (*16*). While the ^{15}N chemical shift tensor orientations with respect to the N–C bond vector have been obtained via ^{15}N–^{13}C REDOR, the orientations of the N–H bond vector in the ^{15}N CSA frame have been obtained from MAS ^{15}N–^{1}H dipolar-shift experiments.

NUMERICAL AND EXPERIMENTAL PROCEDURES

We have employed standard pulse sequences for the recording of ^{15}N CPMAS and ^{15}N–^{1}H dipolar-shift data. In general, iterative fittings of the experimental 1D data, to obtain best-fit values of the parameters of interest, were carried out as in our earlier study (*28*) using the software package "SPINME,"

1090-7807/00 $35.00

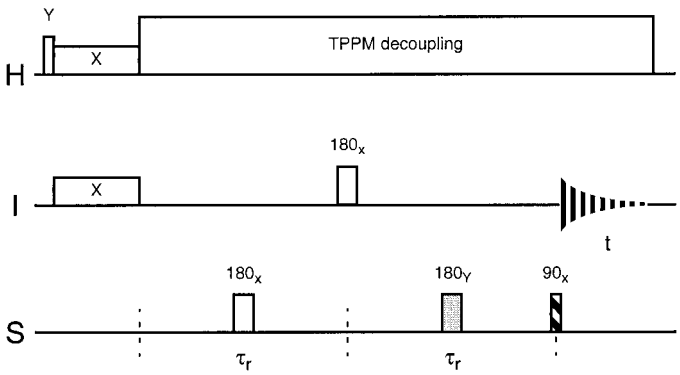

FIG. 1. A two rotor period REDOR pulse sequence with dephasing 180° RF pulses at the center of the rotor periods on the unobserved S channel. The 90° RF pulse on the S channel is employed to purge the signal from contributions from antiphase operator terms which may be present at the start of the data acquisition. Depending on the spinning speed employed the experiment can be carried out with one or two periods of dipolar recoupling by not applying or applying the second 180° pulse on the S spin channel.

which is being developed in-house. In the REDOR study of an isolated and directly coupled ^{15}N–^{13}C spin system a simple one rotor period REDOR sequence with a 180° pulse on the unobserved channel at the center of the rotor period would suffice to obtain orientational information (*28, 29*). However, in multiply labeled systems, one would typically need a two rotor period REDOR sequence (Fig. 1) to eliminate evolution of the observed spins due to isotropic chemical shifts during the REDOR mixing time. Depending upon the spinning speed employed and the heteronuclear dipolar coupling strength in the system under investigation, the two rotor period REDOR experiment can be carried out to achieve significant REDOR dephasing either with one or two rotor periods of dipolar recoupling by executing the REDOR sequence with or without the 180° pulse on the unobserved nuclei during the second rotor period. In this work, REDOR experiments have been carried out with two rotor periods of dipolar recoupling. Considering an isolated I-S spin-1/2 pair, it is seen via standard density matrix calculations that the NMR signal acquired for a single crystallite with two rotor periods of dipolar recoupling as shown in Fig. 1 is given by

$$\langle I^+ \rangle = [\cos 2A \cdot \cos B + \sin 2A \cdot \sin B]\exp(iC), \quad [1]$$

where

$$A = 2D\left(\frac{\omega_{IS}}{\omega_r}\right)\sin \alpha_D, \quad [2]$$

$$B = \frac{\omega_{IS}}{4\omega_r}[2D \sin(\omega_r t - \alpha_D) + G \sin 2(\omega_r t - \alpha_D) + 2D \sin \alpha_D + G \sin 2\alpha_D], \quad [3]$$

and

$$C = \frac{\omega}{2\omega_r} \cdot [(2g_1 \sin \phi_1 + g_2 \sin \phi_2) - (2g_1 \sin(\omega_r t + \phi_1) + g_2 \sin(2\omega_r t + \phi_2))]. \quad [4]$$

In the above equations we have

$$D = 2\sqrt{2} \cdot \sin \beta_D \cdot \cos \beta_D$$

and

$$G = \sin^2 \beta_D,$$

with ω, g_1, g_2, ϕ_1, and ϕ_2 defined as before (*30*). ω_{IS} is the dipolar coupling strength and (β_D, α_D) are the polar and azimuthal angles of the dipolar tensor in the rotor frame. These are given by

$$\cos \beta_D = \cos \theta_D \cdot \cos \beta - \sin \theta_D \cdot \sin \beta \cdot \cos(\gamma + \psi_D),$$

$$\cos(\alpha_D - \alpha) = \frac{\cos \theta_D - \cos \beta \cdot \cos \beta_D}{\sin \beta \cdot \sin \beta_D}.$$

(α, β, γ) are the Euler angles of the CSA in the rotor frame and (θ_D, ψ_D) are the polar and azimuthal angles of the dipole tensor in the CSA frame. A weighted averaging of the response over all possible crystallite orientations gives the final signal observed. The second term in Eq. [1] arises from an antiphase operator term of the type $I_Y S_Z$ present at the start of the data acquisition. Under slow spinning conditions and when one is dealing with significant heteronuclear ^{15}N–^{13}C dipolar couplings comparable to the spinning speed employed, the antiphase operator term can refocus to an observable I_X term during the data acquisition time and can contribute significantly to the observed signal (*29*). The 90° ^{13}C pulse at the start of the data acquisition period shown in Fig. 1 is needed to eliminate the contributions from such terms. The REDOR experiments reported here have been carried out with the application of the 90° purging pulse on the unobserved nuclei. Considering the heteronuclear spins in the system under investigation as two isolated ^{15}N–^{13}C pairs, we have analyzed the REDOR spectra as described earlier (*28*). To assess the error margin in the Euler angles (θ^{exp}, ψ^{exp}) obtained from REDOR spectra we have also carried out an RMSD calculation based on established procedures (*31*). Thus, we calculate and plot the RMSD between the simulated spectrum obtained employing the optimal solution (θ^{exp}, ψ^{exp}) and simulated spectra generated for various values of the angles (θ, ψ) from

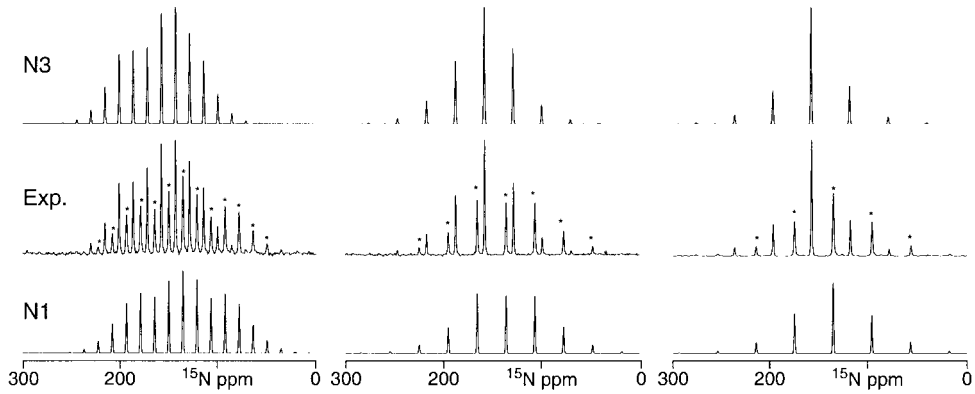

FIG. 2. Experimental (middle row) ^{15}N CPMAS spectra of ^{15}N uracil at spinning speeds of 730 (left), 1500 (middle), and 2000 Hz (right), recorded with 64 (730 Hz) and 32 scans (1500, 2000 Hz), respectively, 64 s of recycle time, and 1 ms of cross-polarization time. The corresponding simulated plots for sites N3 and N1 generated with the optimized CSA parameters given in Table 1 are given above and below the experimental spectra. The signals from the N1 site are indicated with an asterisk in the experimental spectra.

$$\mathrm{RMSD}(\theta, \psi) = \{1/N \sum_{i}^{N} [S_i^{\mathrm{exp}}(\theta^{\mathrm{exp}}, \psi^{\mathrm{exp}}) - S_i^{\mathrm{sim}}(\theta, \psi)]^2\}^{1/2}. \quad [5]$$

$S_i^{\mathrm{exp}}(\theta^{\mathrm{exp}}, \psi^{\mathrm{exp}})$ is the normalized ith sideband intensity of the spectrum obtained from simulations employing the optimal solution $(\theta^{\mathrm{exp}}, \psi^{\mathrm{exp}})$ derived from the experimental data. $S_i^{\mathrm{sim}}(\theta, \psi)$ is the sideband intensity obtained from simulations employing the angles (θ, ψ). N is the total number of sidebands employed in the calculation. From the measured experimental RMS noise, the uncertainty in the evaluated angles $(\theta^{\mathrm{exp}}, \psi^{\mathrm{exp}})$ has been estimated.

All experiments were performed at room temperature on a 500-MHz wide-bore Varian $^{\mathrm{UNITY}}$INOVA solid-state NMR spectrometer equipped with a 5-mm DOTY supersonic triple-resonance probe. Cross-polarization under Hartmann–Hahn matching conditions was applied and typical ^{1}H, ^{15}N, and ^{13}C 90° pulse widths of 3.8, 9.0, and 4.25 μs were used, respectively. Homonuclear ^{1}H decoupling in the dipolar-shift experiments was achieved by employing a semi-windowless MREV8 sequence (*32*); all other spectra were collected under high-power ^{1}H TPPM decoupling (*33*). Standard pulse sequences were employed for obtaining the ^{15}N CPMAS, ^{15}N–^{1}H dipolar-shift, and ^{15}N–^{13}C REDOR spectra. For an estimation of the ^{13}C–^{15}N dipolar coupling, a purged two rotor cycle REDOR sequence was employed at several spinning speeds to obtain REDOR data with different durations of heteronuclear dipolar recoupling. ^{15}N spectra were referenced indirectly relative to DSS (*34*). Other relevant experimental parameters are given in the figure legends. Labeled $^{15}N_2$ and 2-^{13}C, $^{15}N_2$ uracil samples were obtained from Isotec, Inc. The samples were packed into spherical inserts at the center of the rotor volume to provide good H_1 homogeneity throughout the sample volume. The total amount of sample was approx. 10 mg.

RESULTS AND DISCUSSION

Figure 2 shows the 1D ^{15}N CPMAS data obtained employing a ^{15}N-labeled sample of uracil and the corresponding simulated plots generated employing optimized values of the chemical shift tensor parameters (Table 1) estimated via an iterative fitting of the experimental data. Resonances were assigned to the two sites as in the literature (*12*). In Fig. 3, experimental ^{15}N–^{13}C REDOR data obtained at different spinning speeds using the sequence given in Fig. 1 are shown. Iterative fitting of the REDOR data, keeping the N–C dipolar coupling also as a variable, leads to a best-fit dipolar coupling of 960 Hz together with the $(\theta_{\mathrm{NC}}, \psi_{\mathrm{NC}})$ angles given in Table 1. Employing these values and the ^{15}N CS tensor values given in Table 1 we have obtained the simulated REDOR spectra also shown in Fig. 3. The N–C dipolar coupling value employed in our REDOR simulations is smaller than the value of ~1225 Hz reported earlier (*12*). However, a measurement of the dipolar coupling strength from a plot of the ratio of the REDOR difference to full echo intensity, $\Delta S/S_0$ (*22*), as a function of the REDOR dephasing time, Fig. 4, gives a N–C dipolar coupling strength of approximately 1020 Hz and this is in reasonable agreement with the value employed in our simulations. To obtain a measure of the uncertainty in the estimated angles, we have carried out an RMSD calculation as described before. From the RMSD plots shown in Fig. 5, we find the polar and azimuthal angles of orientation of the ^{15}N–^{13}C dipolar vectors in the ^{15}N CSA frame to be in the range of (92 ± 10°, 100 ± 5°) and (132 ± 3°, 88 ± 10°) for the N1 and N3 sites, respectively. It is worth mentioning that even if we fix the N–C dipolar coupling used in the iterative fitting routine to a value of 1020 Hz, the $(\theta_{\mathrm{NC}}, \psi_{\mathrm{NC}})$ angles thus estimated do not differ significantly from the above values and are well within the error range given above (however, the quality of the fit between the experimental data and that obtained from simulations employing a N–C dipolar coupling of 1020 Hz is not as good

TABLE 1
Experimentally Obtained ^{15}N CS Tensor Parameters of Uracil

	CPMAS			REDOR		Dipolar-shift	
ν_r [Hz]	σ_{11} [ppm]	σ_{22} [ppm]	σ_{33} [ppm]	θ_{NC} [°][a]	ψ_{NC} [°][a]	θ_{NH} [°][a]	ψ_{NH} [°][a]
N3							
730	93.9	155.8	223.7	—	—	—	—
1500	94.0	154.4	224.9	132	90	0	—
1600	—	—	—	133	90	15[b]	90[b]
1615	93.8	154.4	225.2	—	—	0	—
1700	—	—	—	132	82	—	—
1800	93.8	155.1	224.5	—	—	0	—
2000	94.3	154.1	225.0	—	—	0	—
Mean[e]	94.0 ± 0.2	154.8 ± 0.8	224 ± 0.7	132 ± 3[c]	88 ± 10[c]	15 ± 5[d]	90 ± 10[d]
N1							
730	49.7	141.7	216.0	—	—	—	—
1500	47.5	142.0	217.9	95	102	0	—
1600	—	—	—	90	102	15[b]	−80[b]
1615	47.9	142.7	216.8	—	—	0	—
1700	—	—	—	90	96	—	—
1800	47.2	143.1	217.1	—	—	0	—
2000	47.8	141.2	218.4	—	—	0	—
Mean[e]	48.0 ± 1.2	142.1 ± 0.9	217.2 ± 1.1	92 ± 10[c]	100 ± 5[c]	15 ± 5[d]	−80 ± 10[d]

[a] $(180 - \theta_{NC})$, $(180 - \theta_{NH})$, $-\psi_{NC}$, $\pm(180 - \psi_{NC})$, $-\psi_{NH}$, and $\pm(180 - \psi_{NH})$ are also allowed solutions.
[b] Determined from 2D DIPSHIFT spectrum.
[c] Error range estimated from REDOR RMSD plots.
[d] Possible error range seen from 2D DIPSHIFT simulations.
[e] Mean values are given for all parameters except for θ_{NH}, which is based only on the 2D DIPSHIFT data (see text).

as obtained with 960 Hz). We have also carried out purged REDOR experiments at a spinning speed of 730 Hz with one rotor period of dipolar recoupling (data not shown) and although the spectral quality is poor the REDOR pattern fits reasonably well with the angles obtained at higher spinning speeds with two rotor periods of dipolar recoupling.

To obtain the orientation of the ^{15}N–^{1}H vector in the ^{15}N CSA frame, we have carried out both 1D and 2D dipolar-shift experiments. In Fig. 6, representative 1D experimental dipolar-shift data obtained at 1800 Hz (data at 1500, 1600, and 2000 Hz not shown) employing the ^{15}N-labeled sample of uracil are given. From an iterative analysis of the 1D dipolar-shift data a

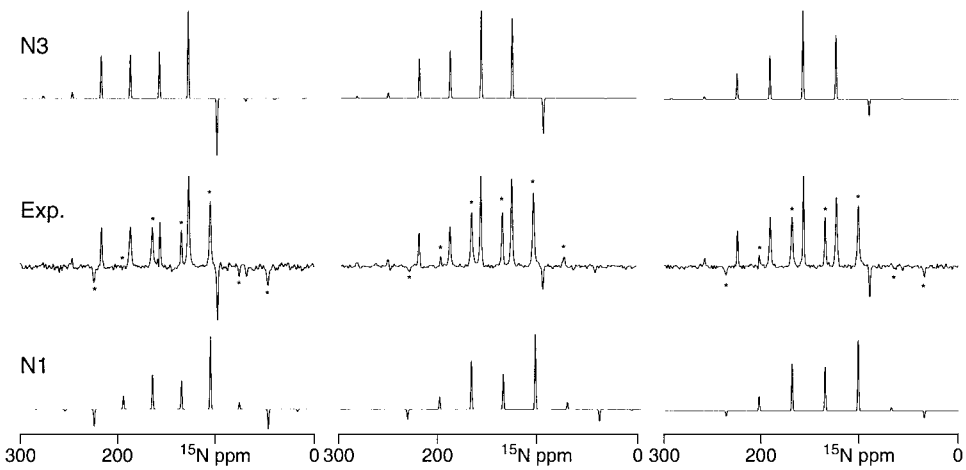

FIG. 3. Experimental (middle row) ^{15}N–^{13}C REDOR spectra of uracil and the corresponding simulated spectra for sites N3 and N1, obtained by employing optimal (θ_{NC}, ψ_{NC}) values given in Table 1 at spinning speeds of 1500 (left), 1600 (middle), and 1700 Hz (right). Mean CSA values given in Table 1 and a dipolar coupling of 960 Hz were used in the simulations. Experiments were carried out using 1200 scans and 64 s of recycle time.

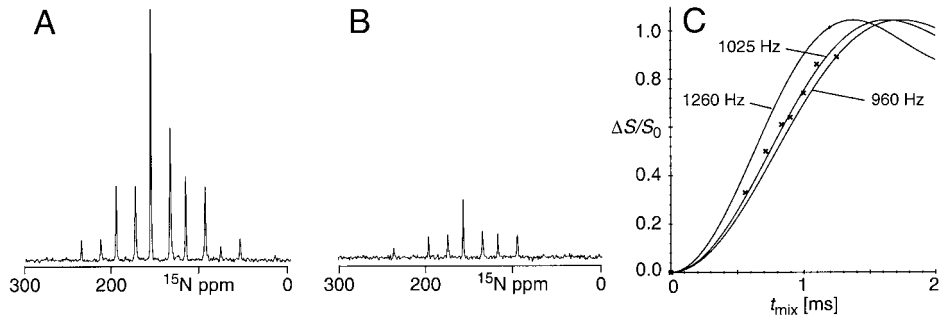

FIG. 4. Example of experimental REDOR spectra at $\nu_r = 2000$ Hz obtained without (A) and with (B) the application of the 180° dephasing pulses on the unobserved channel employing a purged two rotor period REDOR sequence. (C) Experimentally measured $\Delta S/S_0$ as a function of the dipolar recoupling time. Different durations of dipolar recoupling were achieved by varying the spinning frequency ν_r. The simulated continuous REDOR curves were generated assuming the dipolar couplings indicated. $\Delta S/S_0$ showed virtually no difference between N3 and N1, therefore only data points for N3 are shown.

scaled N–H dipolar coupling of 4800 Hz and a θ_{NH} value of 0° are obtained. In Fig. 6 we have shown 1D simulated dipolar-shift spectra obtained with a θ_{NH} value of 0°. For comparisons we have also shown the simulated spectra obtained for a couple of different values of θ_{NH}. For a θ_{NH} value of 0° the simulated plot has no dependence on the value of ψ_{NH} and for θ_{NH} values greater than zero the simulated plots shown have been obtained employing the ψ_{NH} values obtained from the 2D DIPSHIFT experiment discussed below. It is seen from the simulated plots that the quality of fit between the experimental 1D spectrum and the simulated spectra generated with a θ_{NH} value of 0° is not perfect. To obtain a more reliable estimate of the θ_{NH}

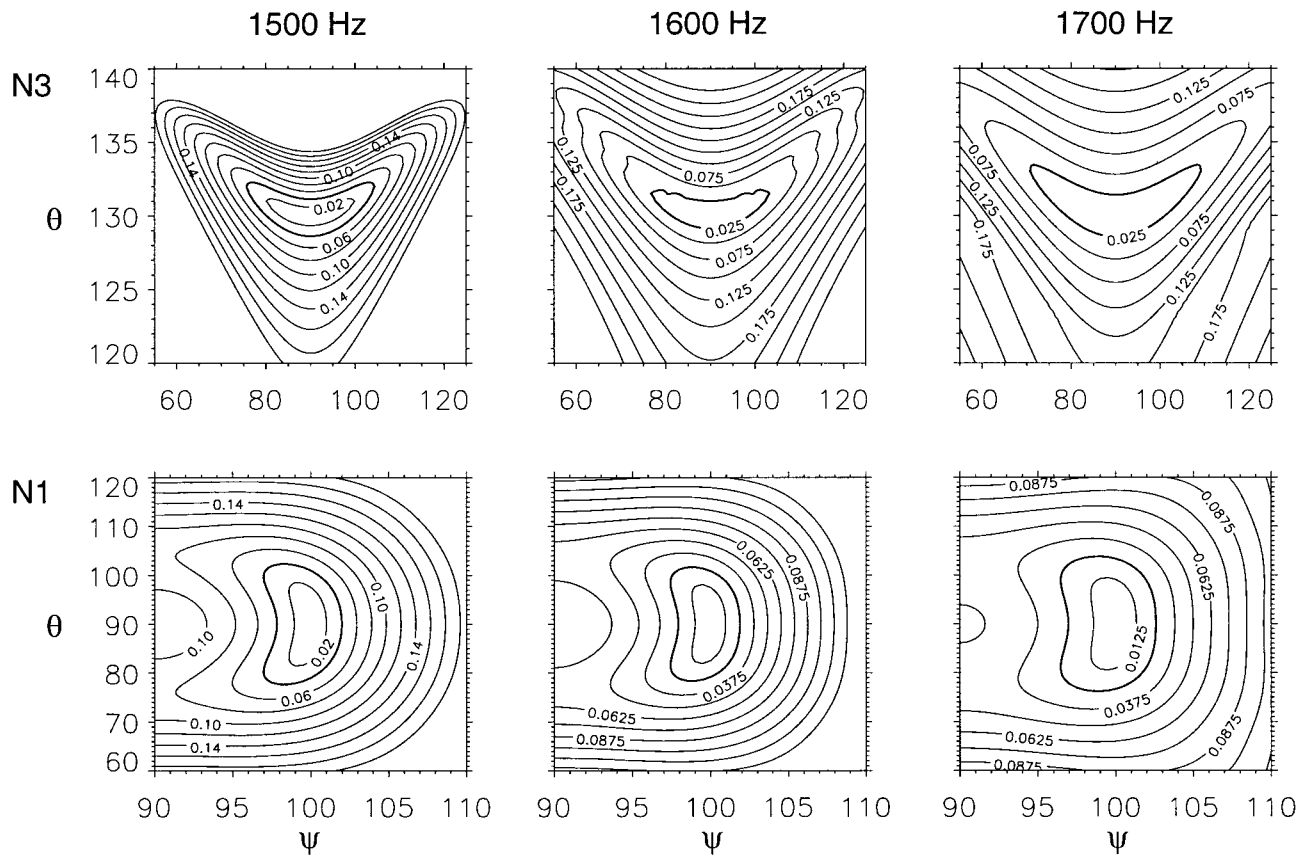

FIG. 5. Plots of the RMSD between the simulated REDOR spectrum obtained employing the angles (θ_{NC}, ψ_{NC}) of (130, 90) and (90, 100) degrees for the N3 and N1 sites, respectively, and simulated spectra generated for various values of (θ, ψ). Mean CSA values given in Table 1 and a dipolar coupling of 960 Hz were used in the simulations carried out at the spinning frequencies indicated. The area enclosed by the thicker contour line, which corresponds to the estimated experimental RMS noise, provides a measure of the uncertainty in (θ_{NC}, ψ_{NC}).

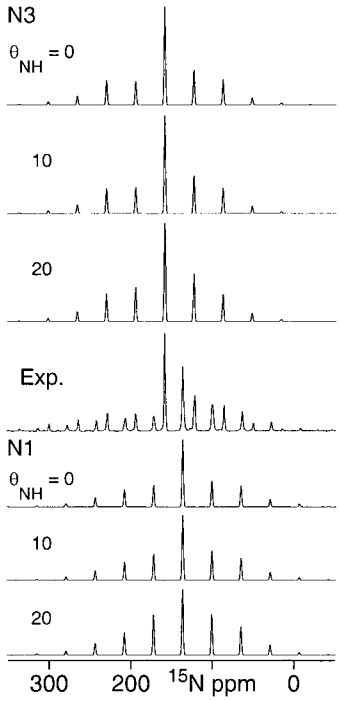

FIG. 6. Experimental MREV8 decoupled ^{15}N CPMAS shift-dipolar spectra at a spinning speed of 1800 Hz and the corresponding simulated plots for sites N3 and N1 as a function of the dipolar vector orientation θ_{NH} assuming a ψ_{NH} value of $+90°$ (N3) and $-80°$ (N1). The simulated plots were obtained employing a scaled dipolar coupling of 4800 Hz (obtained from the fitting procedure) and mean CSA values given in Table 1. Experiments were carried out using 32 scans and 64 s of recycle time.

values, we have carried out a 2D DIPSHIFT experiment and the corresponding spectrum at a spinning speed of 1600 Hz is given in Fig. 7. The optimal values for the N–H vector orien-

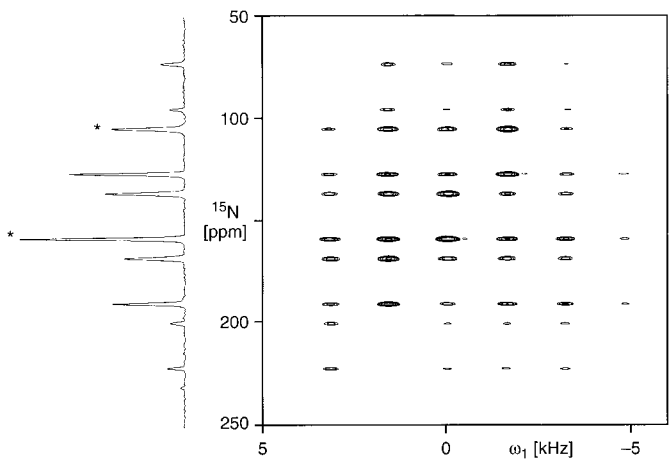

FIG. 7. Two-dimensional phase-sensitive ^{15}N–^{1}H DIPSHIFT spectrum of ^{15}N-labeled uracil at a spinning speed of 1600 Hz. The data were obtained as per the method of Munowitz and Griffin (*27*), which permits the collection of 2D data sets with normal and reversed dipolar evolution in the t_1 dimension. Data acquisition after CP was begun after 16 rotor periods.

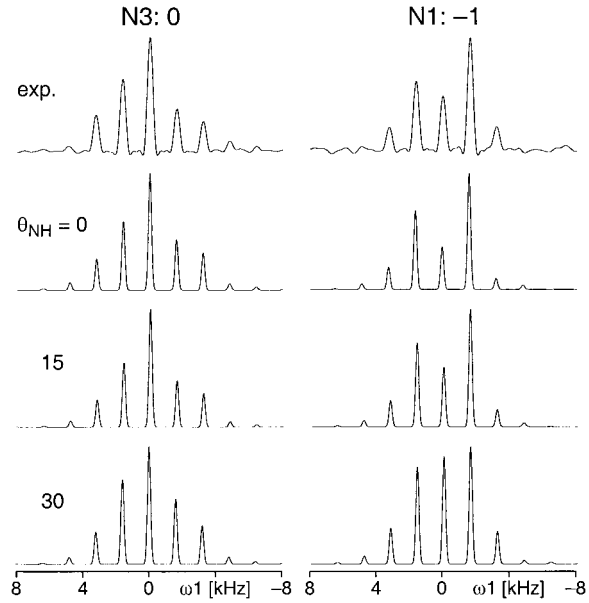

FIG. 8. 2D experimental (top) DIPSHIFT cross sections parallel to ω_1 running through the centerband and sideband resonances in ω_2, as indicated in Fig. 7, of N3 and N1, respectively. The corresponding simulated 2D cross sections as a function of θ_{NH} are given below. The simulated plots were generated assuming a ψ_{NH} value of $+90°$ (N3) and $-80°$ (N1) and a best-fitting scaled dipolar coupling of 4800 Hz.

tation were estimated from the 2D DIPSHIFT spectra by generating several simulated 2D spectra with different values for θ_{NH} and ψ_{NH}. The dipolar coupling strengths were also varied in these simulations and an optimal scaled N–H dipolar coupling of 4800 Hz was found together with the (θ_{NH}, ψ_{NH}) values given in Table 1. The best fitting values for (θ_{NH}, ψ_{NH}) were obtained from that spectrum in which all the cross sections matched reasonably well with the experimental ones, as seen by visual inspection. At this stage of our work, the error range given for the (θ_{NH}, ψ_{NH}) values in Table 1 is only an approximate measure of the accuracy to which the angles could be estimated by the visual comparison of the simulated and experimental 2D dipolar cross sections. In Fig. 8, we give the experimental cross sections (marked in Fig. 7, N3: 0, N1: -1) together with simulated plots obtained with different θ_{NH} values, for the ψ_{NH} values indicated. It is seen that the fit between the experimental and simulated plots is reasonably good with $\theta_{NH} = 15°$ and this value is also consistent with the θ_{NC} values given in Table 1 as the N–C and N–H vectors, which are in the molecular plane, include an angle of $\sim$115° (*35*). In view of this we did not consider the 1D data in the final estimation of θ_{NH} and ψ_{NH} values (Table 1). For (θ_{NC}, ψ_{NC}) values of N1:(92, 100) and N3:(132, 88) degrees and making use of the H–N–C angle of $\sim$115° given in the literature (*35*), one finds the corresponding (θ_{NH}, ψ_{NH}) values to be (15, 90) and (15, -80) degrees. For these values of the angles, the orientation of the ^{15}N CS tensor in uracil is seen to be as depicted in Fig. 9 with the σ_{11} axis essentially perpendicular to the molecular plane. Our results

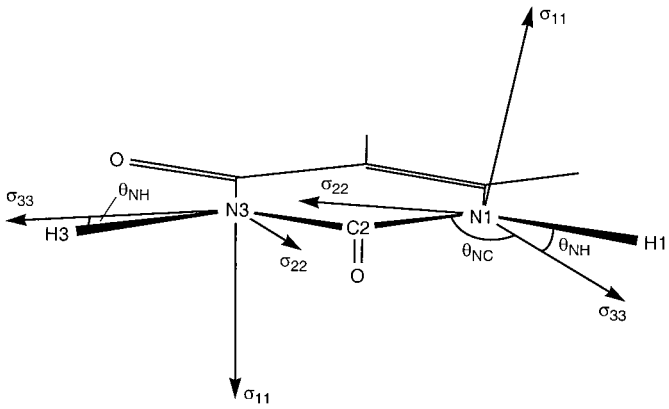

FIG. 9. Orientation of the ^{15}N CSA tensors in the molecular frame of uracil.

are in reasonable agreement with the values reported in the literature (*12*).

This work clearly shows that MAS NMR can possibly be employed for such studies even in multiply labeled polycrystalline specimens. When extensive sideband overlaps make a 1D data analysis difficult, one can possibly take recourse to 2D methods to obtain isotropic chemical shift resolved anisotropic data (*16*). In favorable situations it may be possible to obtain ^{15}N isotropic shift resolved anisotropic data by the very simple 2D rotational spin-echo NMR procedure (*36*). In this the rotor-synchronized sampling of the transverse magnetization generated after CP is followed by data acquisition under high-power heteronuclear or homonuclear ^{1}H decoupling; Figure 10 shows two examples of such spectra in uracil. To obtain isotropic chemical shift resolved REDOR data, the REDOR mixing time can be preceded by the rotor-synchronized sampling of the transverse magnetization in the t_1 dimension. Although the rotor-synchronized sampling restricts the bandwidth in the ω_1 dimension to the spinning speed employed, it is advantageous to keep the spinning speed to the minimum required so as to retain a sufficient number of spinning sidebands in the resultant spectra, as these carry the information of interest. It is worth noting that the isotropic chemical shift dispersions seen for backbone amide nitrogens in proteins and for imino nitrogens in nucleic acid bases are only in the typical range of 30–40 ppm. Hence, even at Zeeman field strengths of 11.74 T, which are routinely available now, it may be possible to obtain satisfactory rotational spin-echo NMR data even with moderate or low spinning speeds. Although collection of two-dimensional isotropic resolved anisotropic data is time consuming, one can reduce data collection time by acquiring only a limited number of t_1 increments and then take recourse to linear prediction in t_1 to improve spectral resolution. The possibility of extracting data from multiply labeled systems demonstrated here would also help in avoiding synthesis of multiple systems with different specific labeling.

In conclusion, it is seen that a combined measurement of the orientation of multiple dipolar vectors in the CSA frame of the nuclei of interest can permit, without any other supporting information from other studies, an accurate characterization of the CS tensor orientation in the molecular frame. From the RMSD plots shown in Fig. 5 it is seen that for the same magnitude of experimental RMS noise the uncertainty in the estimated parameters is larger at higher than at lower spinning speeds. In general, it is necessary for accurate estimation of orientational parameters to have spectra with good signal-to-noise ratio, although collection of REDOR data may be time consuming in situations where one is dealing with systems needing long recycle times. We believe that the rather large error range seen for the angles obtained from the REDOR data can be considerably reduced by data collection with much better signal-to-noise ratio per scan. The need to restrict the sample size to a small, central volume of the rotor to avoid H_1 inhomogeneity effects is one of the main reasons for the poor signal-to-noise ratio seen in the REDOR data. Development of suitable procedures for overcoming H_1 inhomogeneity effects

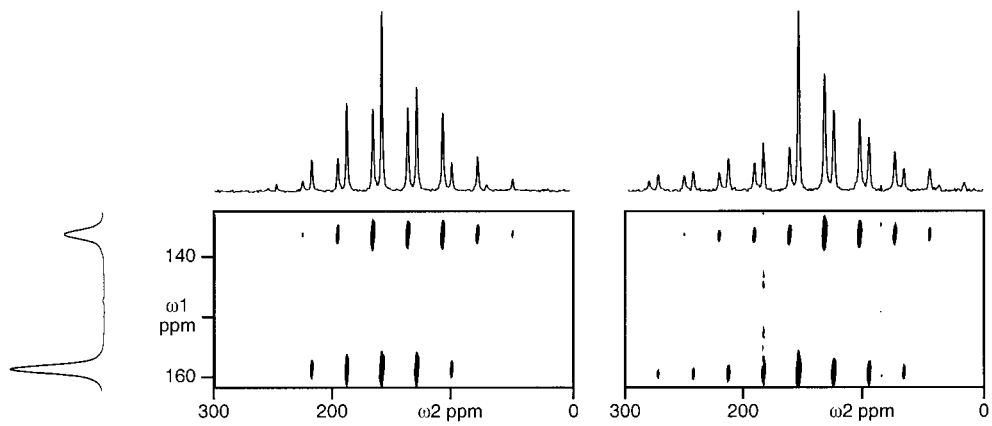

FIG. 10. 2D phase-sensitive isotropic chemical shift resolved CSA (left) and dipolar-shift (right) spectra of $^{15}N_2$-labeled uracil obtained at a spinning speed of 1500 Hz using the rotational spin echo NMR technique (*36*).

would certainly permit the usage of larger sample volumes and thereby facilitate the extraction of orientational parameters with higher precision. Work in this direction is in progress in our laboratory.

It is generally assumed that for the characterization of CS tensors at several sites in a given system one needs multiple compounds with specific labeling at the sites of interest (*37*). This was indeed the approach employed in the previous investigation on uracil via static solid-state NMR methods (*12*). However, this work clearly shows that in favorable situations it may be possible to simultaneously characterize the CS tensors for several sites employing multiply labeled compounds. Similar to the N–C REDOR, one can also carry out a C–N REDOR to obtain the orientation in the molecular frame of the ^{13}C CS tensor. Such works in uracil and other systems are in progress and the results of these studies will be reported elsewhere.

ACKNOWLEDGMENTS

We thank the referees for their valuable comments on our manuscript.

REFERENCES

1. S. J. Opella, P. L. Stewart, and K. G. Valentine, *Q. Rev. Biophys.* **19,** 7 (1987).
2. R. Fu and T. A. Cross, *Annu. Rev. Biomol. Struct.* **28,** 235 (1999).
3. R. G. Griffin, *Nat. Struct. Biol.* **5,** 508 (1998).
4. A. E. Bennett, R. G. Griffin, and S. Vega, "NMR Basic Principles and Progress," Vol. 33, p. 1, Springer-Verlag, Berlin (1994).
5. M. W. F. Fischer, L. Zeng, Y. X. Pang, W. D. Hu, A. Majumdar, and E. R. P. Zuiderweg, *J. Am. Chem. Soc.* **119,** 12629 (1997).
6. D. Yang and L. E. Kay, *J. Am. Chem. Soc.* **120,** 9880 (1998).
7. D. Yang, K. H. Gardner, and L. E. Kay, *J. Biomol. NMR* **11,** 213 (1998).
8. D. Yang, R. Konrat, and L. E. Kay, *J. Am. Chem. Soc.* **119,** 11938 (1997).
9. B. Brutscher, N. R. Skrynnikov, T. Bremi, R. Brüschweiler, and R. R. Ernst, *J. Magn. Reson.* **130,** 346 (1998).
10. A. Shoji, S. Ando, S. Kuroki, I. Ando, and G. A. Webb, *Annu. Rep. NMR Spectrosc.* **26,** 55 (1993).
11. A. C. de Dios and E. Oldfield, *Solid State NMR* **6,** 101 (1996).
12. K. L. Anderson-Altman, C. G. Phung, S. Mavromoustakos, Z. Zheng, J. C. Facelli, C. D. Poulter, and D. M. Grant, *J. Phys. Chem.* **99,** 10454 (1995).
13. J. Z. Hu, J. C. Facelli, D. W. Alderman, R. J. Pugmire, and D. M. Grant, *J. Am. Chem. Soc.* **120,** 9863 (1998).
14. G. A. Lorigan, R. McNamara, R. A. Jones, and S. J. Opella, *J. Magn. Reson.* **140,** 315 (1999).
15. D. Fushman, N. Tjandra, and D. Cowburn, *J. Am. Chem. Soc.* **120,** 10947 (1998).
16. K. Schmidt-Rohr and H. W. Spiess, "Multidimensional Solid State NMR and Polymers," Academic Press, London (1994).
17. C. J. Hartzell, T. K. Pratum, and G. Drobny, *J. Chem. Phys.* **87,** 4324 (1987).
18. M. Bak and N. C. Nielsen, *J. Chem. Phys.* **106,** 7587 (1997).
19. D. M. Gregory, M. A. Mehta, J. C. Shiels, and G. P. Drobny, *J. Chem. Phys.* **107,** 28 (1997).
20. S. Dusold and A. Sebald, *Mol. Phys.* **95,** 1237 (1998).
21. S. Dusold, H. Maisel, and A. Sebald, *J. Magn. Reson.* **141,** 78 (1999).
22. J. M. Goetz and J. Schaefer, *J. Magn. Reson.* **129,** 222 (1997).
23. T. Gullion and J. Schaefer, *J. Magn. Reson.* **81,** 196 (1989).
24. Y. Pan, T. Gullion, and J. Schaefer, *J. Magn. Reson.* **90,** 330 (1990).
25. H. J. M. de Groot, S. O. Smith, A. C. Kolbert, J. M. L. Courtin, C. Winkel, J. Lugtenburg, J. Herzfeld, and R. G. Griffin, *J. Magn. Reson.* **91,** 30 (1991).
26. M. Munowitz, W. P. Aue, and R. G. Griffin, *J. Chem. Phys.* **77,** 1686 (1982).
27. M. Munowitz and R. G. Griffin, *J. Chem. Phys.* **78,** 613 (1983).
28. B. Heise, J. Leppert, and R. Ramachandran, *Solid State NMR* **16,** 177 (2000).
29. J. Leppert, B. Heise, and R. Ramachandran, *J. Magn. Reson.* communicated.
30. J. Leppert, B. Heise, and R. Ramachandran, *J. Magn. Reson.* **139,** 382 (1999).
31. M. Hong, J. d. Gross, W. Hu, and R. G. Griffin, *J. Magn. Reson.* **135,** 169 (1998).
32. W. K. Rhim, D. D. Elleman, and R. W. Vaughan, *J. Chem. Phys.* **59,** 3740 (1973).
33. A. E. Bennett, C. M. Rienstra, M. Auger, K. V. Lakshmi, and R. G. Griffin, *J. Chem. Phys.* **103,** 6951 (1995).
34. D. S. Wishart, C. G. Bigam, J. Yao, F. Abilgaard, H. J. Dyson, E. Oldfield, J. L. Markley, and B. D. Sykes, *J. Biomol. NMR* **6,** 135 (1995).
35. R. K. McMullan and B. M. Craven, *Acta Crystallogr.* **B45,** 270, (1989).
36. W. P. Aue, D. J. Ruben, and R. G. Griffin, *J. Magn. Reson.* **43,** 472 (1981).
37. C. D. Kroenke, M. Rance, and A. G. Palmer III, *J. Am. Chem. Soc.* **121,** 10119 (1999).